Original Article

www.jmss.mui.ac.ir

Computed Tomography Images De-noising using a Novel Two Stage Adaptive Algorithm

Mojtaba Fadaee, Mousa Shamsi, Hamidreza Saberkari[1], Mohammad Hossein Sedaaghi

Department of Electrical Engineering, Sahand University of Technology, Tabriz, [1]Department of Electrical Engineering, Rasht Branch, Islamic Azad University, Rasht, Iran

Submission: 29-08-2015 Accepted: 04-10-2015

ABSTRACT

In this paper, an optimal algorithm is presented for de-noising of medical images. The presented algorithm is based on improved version of local pixels grouping and principal component analysis. In local pixels grouping algorithm, blocks matching based on L^2 norm method is utilized, which leads to matching performance improvement. To evaluate the performance of our proposed algorithm, peak signal to noise ratio (PSNR) and structural similarity (SSIM) evaluation criteria have been used, which are respectively according to the signal to noise ratio in the image and structural similarity of two images. The proposed algorithm has two de-noising and cleanup stages. The cleanup stage is carried out comparatively; meaning that it is alternately repeated until the two conditions based on PSNR and SSIM are established. Implementation results show that the presented algorithm has a significant superiority in de-noising. Furthermore, the quantities of SSIM and PSNR values are higher in comparison to other methods.

Key words: *Computed Tomography Images, Noise, Algorithms, Principal Component Analysis, Signal-to-Noise Ratio*

INTRODUCTION

Computed tomography (CT) scanning is a method that can provide images containing thin sections from the body or other objects.[1] This way of studying inside the objects is used widely in medical science nowadays. In CT scanning, a series of rays (X-rays) are radiated to the sample, and the outgoing ray value is measured. The intensity of the outgoing ray is lower than the radiated ray which is absorbed by the object. In CT scanning, images of horizontal sections of the object are provided two-dimensionally. In these images, Inner parts of the object are displayed as gray levels between black and white, depending on the type and location and the weakening level. To form CT scan images, there are three common stages generally in all systems, which are data acquisition, image reconstruction, and image display. The purpose of data acquisition is to determine the location of each spot in the object and also the CT number of it. To reconstruct and display the image, some matrixes are considered which are formed of square shape small parts and are called pixels. Given that, in CT scanning the image, section or cutting has a thickness. Taking into account the cutting thickness, a volumetric image of each pixel forms a rectangular cube, which is called voxel volume fraction and the section that enfolds all the pixels in a plate, is named slice.[2] Several factors are involved in the quality of CT images:[3]

- Image contrast: It is defined as the difference between CT number of an object and the CT number of its surrounding environment. In fact, it is the difference between density of the object and its surrounding environment
- Spatial resolution: Means the detection and differentiation capability of small components that are close together
- Sensitivity in the direction of the Z-axis: This parameter is effective in the reconstruction of three-dimensional images. Hence that the differentiation of small parts from each other is in the direction of this axis
- Noise: It is the most important factor in CT images which is defined as CT number change in the image of a homogenous object.

Address for correspondence:
Hamidreza Saberkari, Department of Electrical Engineering, Rasht Branch, Islamic Azad University, Rasht, Iran.
E-mail: saberkari@iaurasht.ac.ir

How to cite this article: Fadaee M, Shamsi M, Saberkari H, Sedaaghi MH. Computed Tomography Images De-noising using a Novel Two Stage Adaptive Algorithm. J Med Sign Sense 2015;5:220-9.

A variety of noise sources that cause the destruction of medical images, particularly CT images, are normally approximated as Gaussian white noise.[1] There are several algorithms in references to eliminate Gaussian noise in medical images. In,[4] thresholding method using wavelet transform has been applied which was suggested by Donoho and Johnstone. In this method, wavelet transform coefficients are first extracted. These coefficients are indicators of changes of a particular resolution in a time interval. By considering time intervals in different resolutions, noise in an image can be removed. Thus, thresholding method with wavelet transform includes image catalysis into wavelet coefficients, comparison of details of coefficients, thrseholding to reduce these coefficients, using inverse wavelet transform on improved coefficients to reconstruct images. Choosing threshold limit value plays an important role in de-noising. There are a lot of methods introduced in references for thresholding wavelet transform, which depends on the threshold limit value. Some of these methods are: VisuShrink, SureShrink and BayesShrink.[4-6]

In traditional methods of de-noising, the processing was performed on all pixels. However, in new methods, each image is catalyzed into patches, and the processing is performed on these patches. The main advantage of using these methods is keeping geometrical features and image texture. One of the most popular methods is blocks matching and three-dimensional (BM3D) filtering, which is referred in.[7,8] The disadvantage of this method is its complex structure. Therefore in,[9] independent components analysis is used for de-noising. This has two main stages:

- Applying principal component analysis (PCA), axes perpendicular to each other are also found in noisy image and patches in the image are catalyzed in line with these axes
- De-noising through zeroing all small coefficients in patches of the noisy image existing in axes perpendicular to each other.

A set of patches of input images in PCA is selected through various methods which are general, global, and local methods.[10] In this paper, an optimal algorithm for de-noising in medical images is proposed. The proposed algorithm is based on an improved version of local pixels grouping and PCA. In local pixels grouping algorithm, blocks matching based on L^2 norm method is used, which improves matching performance. The proposed algorithm has two stages, de-noising, and cleanup. The cleanup stage is performed comparatively, which means it is repeated alternately until the two conditions based on structural similarity (SSIM) and peak signal to noise ratio (PSNR) are established.

The rest of the paper is organized as follows: In Section II, a block diagram of the proposed algorithm is raised, and its stages are explained. In Section III, implementation results are given. The majority of implementation results were performed on the CT images. However, to study the stability of the proposed algorithm, we also used some magnetic resonance imaging (MRI) images. Two sets of tests were performed; in the first test, de-noising algorithms in references are first compared, and thee best algorithm is selected based on evaluation criteria. In the second test, the performance of the proposed algorithm is compared to other methods (including the best method selected from the first test). Eventually, Section IV includes a summary of the article.

PROPOSED ALGORITHM

Figure 1 shows the block diagram of the proposed algorithm. As it can be seen, the algorithm has two steps; the first step gives an initial estimate of the image after de-noising. In the next step, noises in the image which still remain are cleaned. In images with high noise, the proposed algorithm removes most of the noises in the first step. However, firm images remain in the images. Therefore, the importance of cleanup step is determined. Cleanup step removes the remained noises and causes the output de-noised images to have a more appropriate quality.

Local Pixels Grouping Algorithm and Principal Component Analysis

Assume that white Gaussian noise υ, with a standard deviation of σ, destructs the original noiseless image I. In

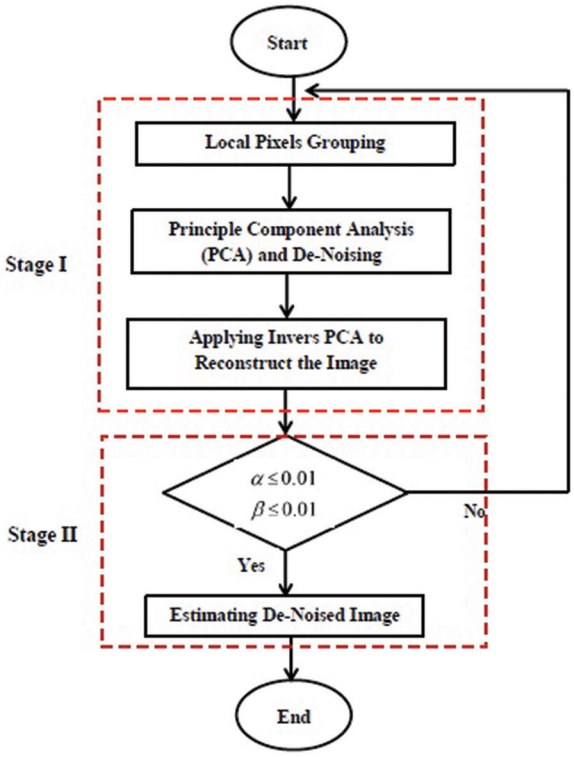

Figure 1: Block diagram of the proposed algorithm

this case, the equation $I_\upsilon = I + \upsilon$ is true about it, which I_υ is the noisy image, υ and I is independent from each other. The purpose of local pixels grouping algorithm is to estimate the de-noised image $\hat{I}$ which must be close to the original image I. Image pixels are specified with brightness value and spatial location. Most of the information of an image is transferred by the structure and one of the crucial factors in images de-noising process is preserving edges. In this method, a pixel and its neighboring pixels are modeled as vector variable and de-noising process is performed on the matrix instead of signal. Figure 2 displays pixels of an image. To de-noise the pixels, we choose the $K \times K$ window in its center and represent it with the vector $X = [x_1 \ x_2 \ \cdots \ x_m]^T$. In this equation, $m = K^2$ is chosen. This vector includes all components inside the window. Thus based on Eq. 1 we have:

$$X_\upsilon = X + \upsilon \tag{1}$$

Where, $X_\upsilon = \left[x_1^\upsilon \ x_2^\upsilon \ \cdots \ x_m^\upsilon\right]^T$, $\upsilon = [\upsilon_1 \ \upsilon_2 \ \cdots \ \upsilon_m]^T$ and $x_K^\upsilon = x_K + \upsilon \rightarrow K = 1,2,...,m$. To estimate X from X_υ, which are noiseless and noisy vector respectively, PCA can be used.

To de-noise X_υ, using PCA, we require training samples of X_υ to compute covariance matrix and principal component transform matrix. For this purpose, we use training block $L \times L$ ($L > K$) to find training samples which are in the center of X_υ. The simplest way to find training samples from noisy variable X_υ is to select all pixels of the block $K \times K$; but in this method, $(L-K+1)^2$ training samples are obtained in total for each component x_K^υ from X_υ. Choosing this set as training samples would be different from selecting all pixels in training block $K \times K$; because selecting all pixels in training block $K \times K$ causes inaccurate estimation of covariance matrix X_υ, and as a result inaccurate estimation of principal component matrix. This increases noise amount in the de-noised image. Thus, selecting and grouping training samples to perform PCA is essential. In the next section, the grouping method used in this article is expressed.

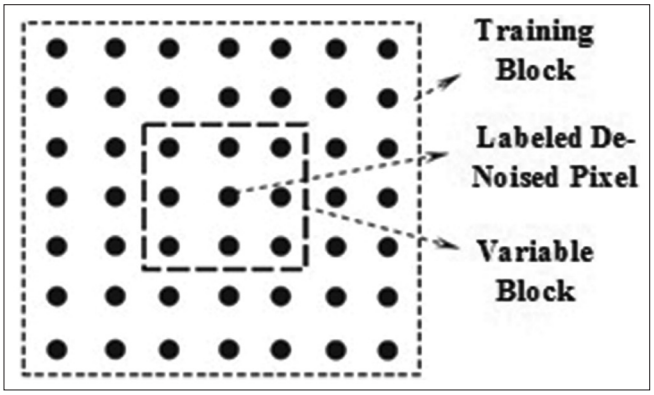

Figure 2: Modeling of local pixels grouping algorithm and principal component analysis in it

Local Pixels Grouping

As mentioned, training samples grouping includes choosing central block $K \times K$ inside the training window $L \times L$. There are a lot of methods proposed in references for classification, which some of them are: Clustering with k^{th} average,[11] fuzzy logic clustering,[12] vector quantization[13] and blocks matching. In this paper, blocks matching method is used in order to group local pixels. As noted before, there are $(L-K+1)^2$ training samples from X_υ in total in training window $L \times L$. Suppose that $\vec{x}_o^\upsilon$ is an indicator of a column vector of the sample containing pixels in the central block $K \times K$, and $\vec{x}_i^\upsilon$ an indicator of samples vectors in accordance with the other blocks, which $i = 1,2,...,(l-k+1)^2 - 1$. Furthermore, assume that $\vec{x}_o$ and $\vec{x}_i$ are noiseless vectors of $\vec{x}_o^\upsilon$ and $\vec{x}_i^\upsilon$. We have:

$$e_i = \frac{1}{m}\sum_{k=1}^{m} \vec{x}_o^\upsilon(k) - \vec{x}_i^\upsilon(k)^2 \approx \frac{1}{m}\sum_{k=1}^{m} \vec{x}_o(k) - \vec{x}_i(k)^2 + 2\sigma^2 \tag{2}$$

Which the noise υ, is Gaussian white noise independent from the signal. According to Eq. 2, in the case of establishing the condition $e_i < T + 2\sigma^2$, $\vec{x}_i^\upsilon$ can be chosen as a vector sample of $\vec{X}_\upsilon$. In this equation, T is the thresholding value. Assume that we select n vector sample of X_υ including central vector $\vec{x}_0^\upsilon$. Central vector samples are demonstrated as $\vec{x}_0^\upsilon, \vec{x}_1^\upsilon, ..., \vec{x}_{n-1}^\upsilon$ and noiseless vectors are considered as $\vec{x}_0, \vec{x}_1, ..., \vec{x}_{n-1}$. Thus, the training data set is represented as $X_\upsilon = \left[\vec{x}_0^\upsilon \ \ \vec{x}_1^\upsilon \ \ . \ . \ . \ \ \vec{x}_{n-1}^\upsilon\right]$ and noiseless data as $X = \left[\vec{x}_0 \ \ \vec{x}_1 \ \ . \ . \ . \ \ \vec{x}_{n-1}\right]$.

Cleanup Stage

There are two main reasons for developing cleanup stage:

- Strong noises existing in X_υ data sets, which leads to inaccurate estimation of covariance matrix and PCA matrix, which reduces efficiency of de-noising algorithm
- Strong noises in main datasets, leads to an error in grouping local pixels.

The input of the cleanup stage is the de-noised image from the first stage. To perform the de-noising process in this stage, the standard deviation of the noise amount in the output image of the first stage should be computed. We have:

$$\hat{I} = I + \upsilon_s \tag{3}$$

Which $\hat{I}$ and υ_s are the output image and the remaining amount of noise from the first stage, respectively. It is essential to approximate the remaining amount of noise ($\sigma_s = \sqrt{E\left[\upsilon_s^2\right]}$) and use it as the cleanup stage input. σ_s is approximated based on the difference between the input

noisy image I_υ in the first stage and the de-noised image $\hat{I}$ in the first stage (the input noisy image in the second stage). Therefore, it can be written as:

$$\tilde{I} = I_\upsilon - \hat{I} = \upsilon - \upsilon_s \tag{4}$$

Based on the above equation, we have:

$$E\left[\tilde{I}^2\right] = E\left[\upsilon^2\right] + E\left[\upsilon_s^2\right] - 2E\left[\upsilon.\upsilon_s\right] = \sigma^2 + \sigma_s^2 - 2E\left[\upsilon.\upsilon_s\right] \tag{5}$$

The noise υ_s contains low-frequency components of υ and we have $\tilde{\upsilon} = \upsilon - \upsilon_s$, so it can be concluded that $\tilde{\upsilon}$ contains high-frequency components of υ. Moreover, according to Eq. 6 we can write:

$$E\left[\upsilon.\upsilon_s\right] = E\left[\hat{\upsilon}.\upsilon_s\right] + E\left[\upsilon_s^2\right] \tag{6}$$

In Eq. 6, the phrase $E\left[\hat{\upsilon}.\upsilon_s\right]$ is much smaller than the phrase $E\left[\upsilon_s^2\right]$. Hence, we can write it as:

$$E\left[v.v_s\right] = E\left[\tilde{v}.v_s\right] + E\left[v_s^2\right] \approx E\left[v_s^2\right] \Rightarrow \sigma_s^2 \approx \sigma^2 - E\left[\hat{I}^2\right] \tag{7}$$

υ_s includes the remaining amount of noise and the noises that were wrongly estimated in the noiseless image *I*. So, we have:

$$\sigma_s = c_s\sqrt{\sigma^2 - E\left[\hat{I}^2\right]} \tag{8}$$

In Eq. 8, we have $c_s < 1$. (c_s is a constant) To find out how many stages are needed to apply for removing Gaussian white noise with different standard deviations, two conditions which are achieved in accordance with Eq. 9, are used.

$$\alpha = \frac{PSNR_{\text{Im}.out} - PSNR_{\text{Im}.in}}{PSNR_{\text{Im}.in}} \times 100$$
$$\beta = \frac{SSIM_{\text{Im}.out} - SSIM_{\text{Im}.in}}{SSIM_{\text{Im}.in}} \times 100 \tag{9}$$

Where, $PSNR_{\text{Im}.out}$ is signal to output noise ratio and $PSNR_{\text{Im}.in}$ is signal to input noise ratio in the same stage. $SSIM_{\text{Im}.out}$ is the structural similarity between the output image and the original image, and $SSIM_{\text{Im}.in}$ is the structural similarity between the input image and the original image. Based on Eq. 9, if $\alpha \leq \%1$ and $\beta \leq \%1$, the cleanup step in the proposed algorithm will be stopped. Otherwise, cleanup steps will continue. In intermediate amounts of noise, in most cases the number of reputation is three. However, in the noises with high standard deviation the number of cleanup steps increases to fulfill the two mentioned conditions.

RESULTS AND DISCUSSION

To evaluate performance of the proposed algorithm in de-noising, the two following evaluation criteria have been used:

Peak Signal to Noise Ratio

PSNR indicates the ratio of maximum possible power to noise power. Because so many signals contain a wide

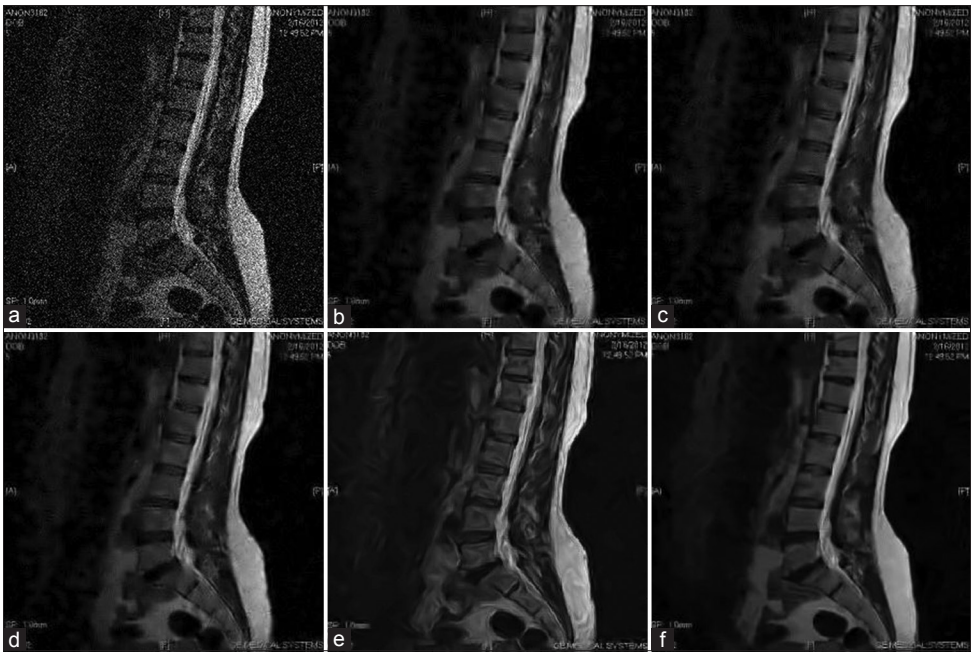

Figure 3: Comparison of results of different algorithms in removing Gaussian white noise from magnetic resonance imaging image of vertebral column, (a) noisy image of vertebral column destructed by white Gaussian noise with standard deviation of σ = 36, (b) de-noising using patch-based global principal component analysis method, (c) de-noising using patch-based local principal component analysis method, (d) de-noising using patch-based hierarchical principal component analysis method, (e) de-noising using locally learned dictionaries method and (f) de-noising using the blocks matching and three-dimensional algorithm

dynamic range, this evaluation criterion defined in the form of logarithm. This criterion is used to measure the quality of images after reconstructing them, the higher the criterion amount, the better the quality of the reconstructed image. The signal to noise ratio is expressed as the mean square error. If we show the noiseless image with I and the noisy image with K, based on Eq. 10, we have:[14]

$$MSE = \frac{1}{mn}\sum_{i=0}^{m-1}\sum_{j=0}^{n-1}\left[I(i,j)-K(i,j)\right]^2$$
$$\rightarrow PSNR = 10\log_{10}\left(\frac{MAX_I^2}{MSE}\right) = 20\log_{10}\left(\frac{MAX_I}{\sqrt{MSE}}\right) \quad (10)$$

Where MAX_I is the maximum number of pixels in the image, and if the image pixels were 8-bit, MAX_I will be equal to 255. Otherwise, it is computed using Eq. 11:

$$MAX_I = 2^B - 1 \quad (11)$$

Structural Similarity

This criterion is a method to measure the similarity between two images and is defined as:[15,16]

$$SSIM(x,y) = \frac{\left(2\mu_x\mu_y + c_1\right)\left(2\sigma_{xy} + c_2\right)}{\left(\mu_x^2 + \mu_y^2 + c_1\right)\left(\sigma_x^2 + \sigma_y^2 + c_2\right)} \quad (12)$$

Where, μ_x and μ_x is the average of x and y, σ_x^2 and σ_y^2 is the variance of x and y, respectively. σ_{xy} is the covariance between x and y. c_1 and c_2 are two variables which is defined as, $c_1 = (k_1 l)^2, c_2 = (k_2 l)^2$, respectively. The values of k_1 and k_2 are chosen as 0.01 and 0.03. Also, l is the number of bits of the pixel.

Experiment I: Evaluation of some algorithms for De-noising

In this article, locally learned dictionaries,[17] patch based global PCA (PGPCA),[10,18] patch based local PCA,[9] patch based hierarchical PCA[10] and BM3D[19] methods are implemented with the purpose of comparison. In Figure 3, results of applying algorithms available in references to remove Gaussian white noise on vertebral column MRI image are shown. As can be seen, BM3D algorithm has greater ability in de-noising than other methods. The reason is using two block matching steps which is done based on the distance between blocks in the first blocks matching step, and based on normalization or L^2 norm in the second step. However, the main issue in this algorithm is its high computational complexity which leads to high execution time. The reason is BM3D uses two level of block matching using the block distance and normalization, respectively. In Table 1, the obtained values of PSNR for different standard deviations for all kinds of medical images are given. Furthermore, In Figure 4, PSNR diagram is plotted according to standard deviation.

Table 1: Quantitative comparison of PSNR of different algorithms in removing Gaussian white noise for choosing different SD amounts

Medical images	De-nosing method				
	K-LLD[17]	PGPCA[10]	PLPCA[9]	PHPCA[10]	BM3D[19]
PSNR (σ=6)					
Abdomen	37.64	39.00	39.41	39.03	40.26
Chest	38.47	38.43	39.06	38.77	39.63
Brain	35.89	37.03	37.14	36.94	38.11
Liver	36.59	38.11	38.32	39.07	38.55
Spine	37.88	38.22	38.31	38.25	38.82
PSNR (σ=12)					
Abdomen	33.64	34.84	35.31	34.99	36.87
Chest	34.91	34.22	34.90	34.68	36.02
Brain	31.00	32.35	32.61	32.45	33.55
Liver	33.39	34.27	34.50	34.27	35.19
Spine	34.11	33.43	33.86	33.80	34.83
PSNR (σ=18)					
Abdomen	30.93	32.70	33.21	32.98	34.86
Chest	32.84	31.94	32.70	32.53	33.99
Brain	28.74	29.91	30.28	30.14	31.20
Liver	31.12	32.34	32.65	32.49	33.49
Spine	31.40	31.17	31.33	31.25	32.45
PSNR (σ=24)					
Abdomen	28.77	30.97	31.46	31.32	33.37
Chest	31.23	30.28	30.94	30.83	32.48
Brain	27.03	28.37	28.75	28.63	29.73
Liver	29.28	30.94	31.14	31.07	32.29
Spine	29.44	29.25	29.52	29.45	30.74
PSNR (σ=30)					
Abdomen	27.02	29.68	30.12	30.02	32.18
Chest	29.90	29.01	29.59	29.51	31.33
Brain	25.56	27.21	27.61	27.52	28.68
Liver	27.67	29.87	29.92	29.91	31.30
Spine	27.65	28.05	28.13	28.11	29.43
PSNR (σ=36)					
Abdomen	25.47	28.65	29.04	28.93	31.08
Chest	28.54	27.99	28.50	28.45	30.38
Brain	24.29	26.33	26.70	26.61	27.76
Liver	26.16	28.97	28.98	28.98	30.43
Spine	26.05	27.05	27.02	27.05	28.37

SD – Standard deviation; PSNR – Peak signal to noise ratio; K-LLD – Locally learned dictionaries; PCA – Principal component analysis; PGPCA – Patch based global PCA; PLPCA – Patch based local PCA; PHPCA – Patch based hierarchical PCA; BM3D – Blocks matching and three-dimensional filtering

Experiment II: Performance evaluation of the proposed algorithm

In Figure 5, results of applying the proposed algorithm on medical images are shown. These medical images are destructed by Gaussian white noise with standard deviation of $\sigma = 60$. The superiority of the proposed algorithm in de-noising is clearly seen. As mentioned, the reason is using two de-noising and cleanup stages. The cleanup stage also includes some de-noising steps. According to the conditions stated in the proposed algorithm, the number of repeats of the cleanup stages is considered three for all standardized values. In Table 2, the performance of the

proposed algorithm in each stage is displayed. According to this table, it is clear that PSNR and SSIM values in the third stage of cleanup have remarkably improved in comparison to noisy images.

In Figures 6, the comparison of the proposed algorithm and other methods in de-noising in vertebral column MRI images is demonstrated. Furthermore, in diagrams related to Figures 7 and 8, the comparison between our proposed algorithm with other de-noising methods in CT scan images are given for PSNR and SSIM measures. In these figures, the horizontal axis of Gaussian white noise with standard deviations higher than $\sigma = 60$ is for each image. Also, quantitative comparison of PSNR and SSIM values with other methods is given in Table 3. The proposed algorithm has considerably improved in PSNR and also SSIM amount in comparison to classical local pixels grouping algorithm and PCA (without a change in cleanup stages), methods based on PCA, wavelet transform and clustering.

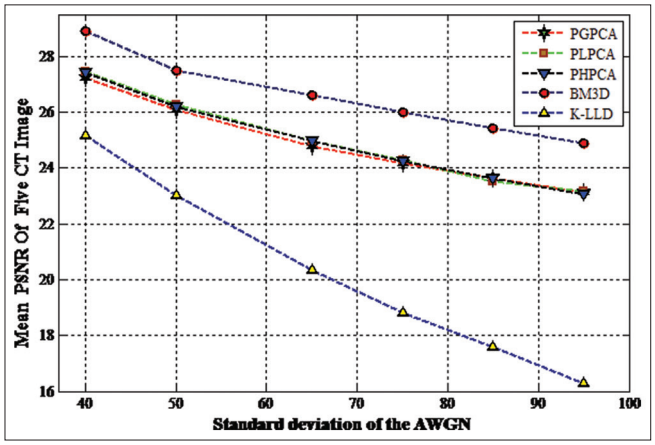

Figure 4: Comparison of peak signal to noise ratio average of different algorithms for choosing different standard deviation amounts on five medical images of abdomen, chest, brain, vertebral column and liver

CONCLUSION

In the field of biomedical image processing, the problem of image de-noising forms a significant preliminary step of image restoration. A major concern in image de-noising models is to preserve important features such as edges and lines which are easily detected by the human visual system while de-noising process. In this paper, a two-stage adaptive algorithm has been proposed for medical images de-noising which was based on the combination of local pixels grouping and principle component analysis model. In the proposed algorithm, block matching has done by L^2 norm method which leads to the better matching performance

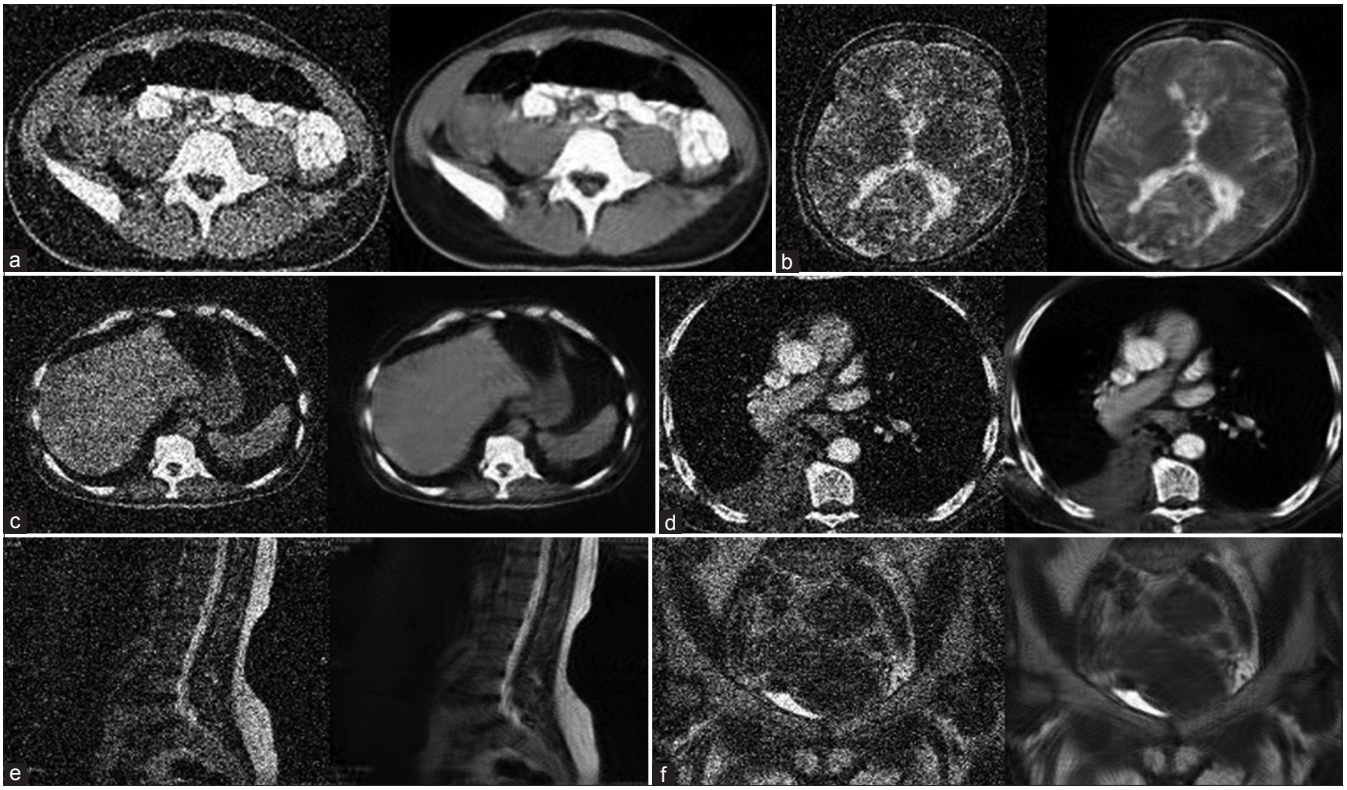

Figure 5: Applying proposed algorithm in removing Gaussian white noise with standard deviation of 60 in images: (a) Abdominal computed tomography scan, (b) brain magnetic resonance imaging, (c) liver computed tomography scan, (d) computed tomography scan of the lungs, (e) vertebral column magnetic resonance imaging and (f) pelvis computed tomography scan

Table 2: Comparison of the proposed algorithm results in different reputations

Medical images	De-noising stages				
	Noisy image	First stage (de-noising)	Cleanup (first step)	Cleanup (second step)	Cleanup (third step)
PSNR (SSIM) for σ=24					
Abdomen	26.52 (0.6525)	26.87 (0.6761)	28.15 (0.7619)	28.41 (0.7810)	28.43 (0.7820)
Brain	26.52 (0.5228)	27.95 (0.6351)	29.60 (0.7992)	29.91 (0.8360)	29.94 (0.8392)
Liver	26.52 (0.5636)	27.85 (0.6559)	29.33 (0.7822)	29.59 (0.8082)	29.61 (0.8108)
Lung	26.52 (0.5461)	27.28 (0.6321)	28.68 (0.7645)	28.94 (0.7945)	28.97 (0.7975)
Spine	26.52 (0.5277)	27.77 (0.6540)	29.18 (0.8006)	29.43 (0.8306)	29.45 (0.8335)
Pelvis	26.52 (0.6398)	27.10 (0.6678)	28.41 (0.7441)	28.67 (0.7600)	28.69 (0.7615)
PSNR (SSIM) for σ=48					
Abdomen	20.49 (0.4372)	22.20 (0.4678)	24.02 (0.5828)	24.40 (0.6198)	24.43 (0.6238)
Brain	20.49 (0.3173)	23.29 (0.3825)	25.57 (0.5765)	26.03 (0.6491)	26.08 (0.6566)
Liver	20.49 (0.3310)	23.25 (0.4140)	25.52 (0.6048)	25.97 (0.6680)	26.01 (0.6750)
Lung	20.49 (0.3444)	22.50 (0.3996)	24.41 (0.5586)	24.78 (0.6120)	24.81 (0.6177)
Spine	20.49 (0.2933)	23.29 (0.3939)	25.38 (0.6149)	25.76 (0.6868)	25.79 (0.6943)
Pelvis	20.49 (0.3641)	22.81 (0.4335)	24.65 (0.5670)	25.00 (0.6012)	25.04 (0.6046)
PSNR (SSIM) for σ=72					
Abdomen	16.98 (0.3194)	19.53 (0.3504)	21.68 (0.4600)	22.14 (0.5037)	22.17 (0.5099)
Brain	16.98 (0.2197)	20.52 (0.2549)	23.23 (0.4072)	23.80 (0.4806)	23.86 (0.4891)
Liver	16.98 (0.2251)	20.49 (0.2866)	23.27 (0.4697)	23.86 (0.5531)	23.91 (0.5634)
Lung	16.98 (0.2495)	19.77 (0.2869)	22.07 (0.4221)	22.53 (0.4814)	22.57 (0.4883)
Spine	16.98 (0.1916)	20.67 (0.2603)	23.39 (0.4727)	23.92 (0.5725)	23.97 (0.5846)
Pelvis	16.98 (0.2280)	20.30 (0.2961)	22.60 (0.4495)	23.04 (0.4978)	23.08 (0.5029)
PSNR (SSIM) for σ=96					
Abdomen	14.48 (0.2434)	17.63 (0.2729)	20.07 (0.3716)	20.58 (0.4131)	20.64 (0.4187)
Brain	14.48 (0.1607)	18.50 (0.1806)	21.62 (0.2953)	22.29 (0.3564)	22.35 (0.3640)
Liver	14.48 (0.1653)	18.47 (0.2114)	21.65 (0.3708)	22.35 (0.4588)	22.41 (0.4706)
Lung	14.48 (0.1918)	17.84 (0.2207)	20.47 (0.3304)	21.00 (0.3857)	21.05 (0.3929)
Spine	14.48 (0.1355)	18.74 (0.1861)	22.00 (0.3691)	22.68 (0.4795)	22.74 (0.4946)
Pelvis	14.48 (0.1541)	18.43 (0.2108)	21.19 (0.3650)	21.72 (0.4238)	21.77 (0.4304)

PSNR – Peak signal to noise ratio; SSIM – Structural similarity

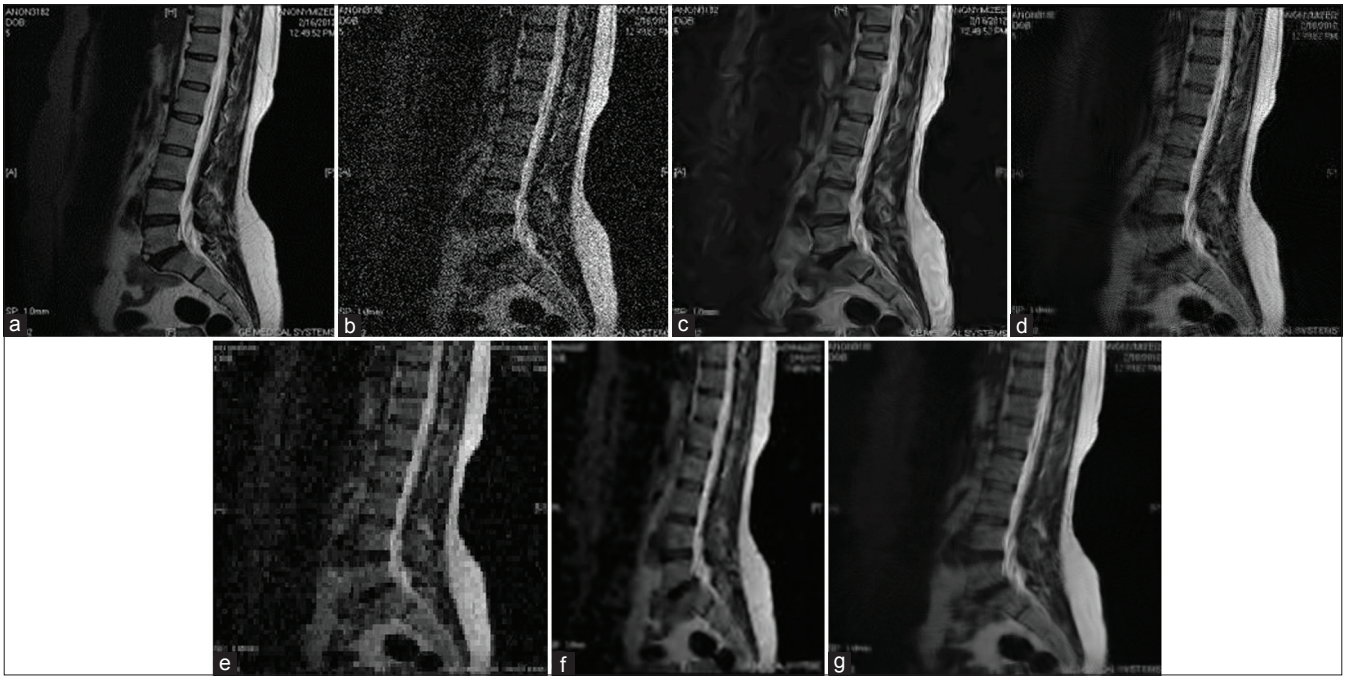

Figure 6: Comparison of different methods for de-nosing vertebral column medical image. (a) Noiseless image. (b) The noisy image destructed by Gaussian white noise with standard deviation of $\sigma = 36$. (c) Locally learned dictionaries method, (d) local pixels grouping-principal component analysis method, (e) Bayes method, (f) patch based global principal component analysis method, (g) the proposed algorithm

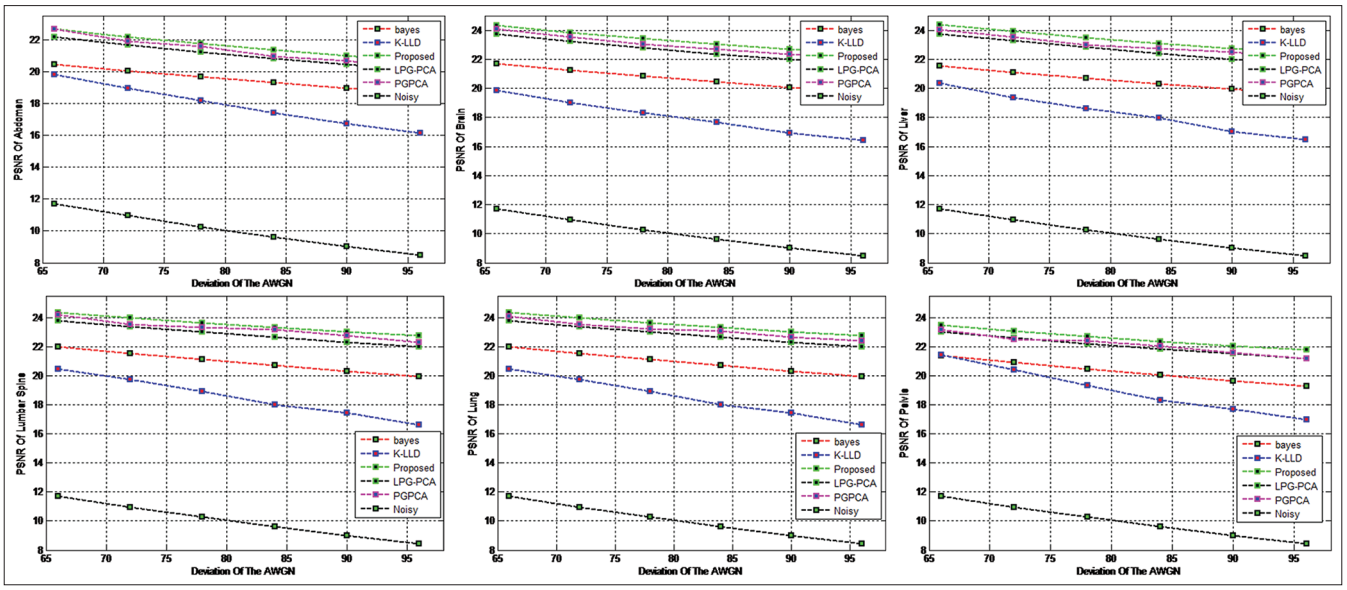

Figure 7: Plot of peak signal to noise ratio versus additive white Gaussian noise with $\sigma = 60$ in proposed algorithm and other de-noising methods in computed tomography scan images

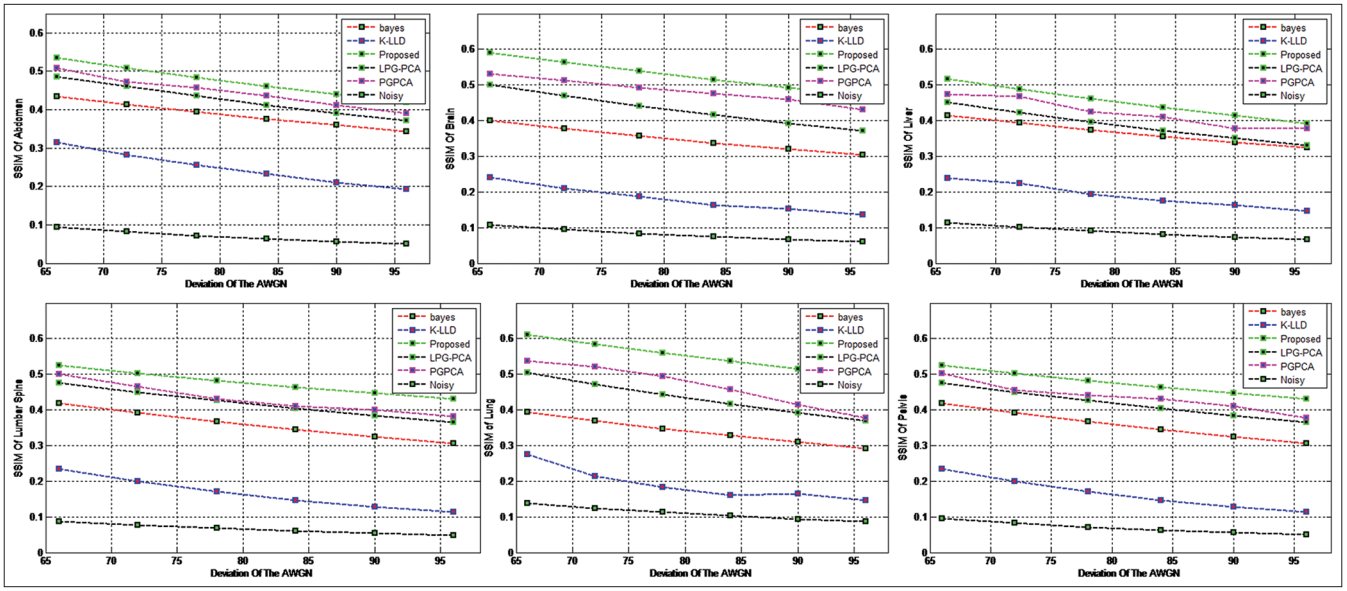

Figure 8: Plot of structural similarity versus additive white Gaussian noise with $\sigma = 60$ in proposed algorithm and other de-noising methods in computed tomography scan images

of local pixels and therefore, we are faced with minimum amount of error in the covariance matrix. The reputation of cleanup stage in our proposed algorithm was selected by two, PSNR and SSIM, measurers.

One of the main features of the proposed algorithm is its robustness against different kind of noise sources which are modeled by additive white Gaussian noise. As can be seen from experimental results, the performance of the algorithm improves by increasing the noise. Our future works focus on utilizing the proposed method in this paper with partial differential equations-based methods (e.g., nonlinear anisotropic diffusion method)[20,21] for further improvements of medical image de-noising.

Financial Support and Sponsorship

Nil.

Conflicts of Interest

There are no conflicts of interest.

Table 3: Comparison of PSNR and SSIM values of different algorithms in comparison to the proposed algorithm with different SDs of Gaussian white noise

Medical images	De-noising method					
	Noisy image	K-LLD[17]	PGPCA[10]	LPG-PCA[9]	Bayes Shrink[5]	Proposed algorithm
PSNR (SSIM) for σ=12						
Abdomen	26.52 (0.6525)	31.94 (0.7632)	32.40 (0.8859)	32.34 (0.8839)	29.90 (0.7803)	32.50 (0.8917)
Brain	26.52 (0.5228)	32.78 (0.6094)	34.09 (0.9266)	33.89 (0.9185)	30.79 (0.7199)	34.11 (0.9319)
Liver	26.52 (0.5636)	32.68 (0.8691)	32.90 (0.8834)	33.12 (0.8944)	30.28 (0.7735)	33.27 (0.9035)
Lung	26.52 (0.5461)	32.64 (0.7293)	33.14 (0.8763)	33.07 (0.8927)	30.34 (0.7592)	33.27 (0.9057)
Spine	26.52 (0.5277)	34.05 (0.9143)	33.43 (0.9136)	33.39 (0.9054)	30.79 (0.7939)	33.58 (0.9164)
Pelvis	26.52 (0.6398)	33.17 (0.9015)	32.53 (0.8885)	32.43 (0.8711)	30.16 (0.8185)	32.61 (0.8772)
PSNR (SSIM) for σ=24						
Abdomen	20.49 (0.4372)	28.21 (0.6543)	28.32 (0.7729)	28.15 (0.7619)	25.68 (0.6515)	28.43 (0.7820)
Brain	20.49 (0.3173)	28.18 (0.4700)	29.75 (0.82050)	29.60 (0.7992)	26.65 (0.5885)	29.94 (0.8392)
Liver	20.49 (0.3310)	29.41 (0.7171)	29.16 (0.6858)	29.32 (0.7822)	26.57 (0.6371)	29.61 (0.8108)
Lung	20.49 (0.3444)	28.35 (0.5623)	28.83 (0.7762)	28.68 (0.7645)	26.13 (0.6302)	28.97 (0.7975)
Spine	20.49 (0.2933)	29.23 (0.7407)	29.25 (0.8049)	29.18 (0.8006)	26.86 (0.6690)	29.45 (0.8335)
Pelvis	20.49 (0.3641)	29.92 (0.7479)	28.62 (0.7513)	28.41 (0.7441)	26.42 (0.6817)	28.69 (0.7615)
PSNR (SSIM) for σ=36						
Abdomen	16.98 (0.3194)	25.49 (0.5372)	25.75 (0.6715)	25.72 (0.6630)	23.42 (0.5697)	26.07 (0.6954)
Brain	16.98 (0.2197)	25.20 (0.3676)	27.25 (0.7125)	27.22 (0.6825)	24.58 (0.5012)	27.66 (0.7470)
Liver	16.98 (0.2251)	26.37 (0.5294)	27.35 (0.6717)	27.11 (0.6880)	24.46 (0.5478)	27.51 (0.7386)
Lung	16.98 (0.2495)	25.00 (0.4483)	26.32 (0.6756)	26.15 (0.6527)	23.73 (0.5502)	26.51 (0.7025)
Spine	16.98 (0.1916)	25.76 (0.5399)	27.05 (0.7267)	26.88 (0.7021)	24.79 (0.5671)	27.23 (0.7591)
Pelvis	16.98 (0.2280)	27.47 (0.5518)	27.52 (0.6501)	26.16 (0.6452)	24.38 (0.5890)	25.51 (0.6732)
PSNR (SSIM) for σ=48						
Abdomen	14.48 (0.2434)	22.97 (0.4336)	24.15 (0.5964)	24.02 (0.5828)	21.98 (0.5073)	24.43 (0.6238)
Brain	14.48 (0.1607)	22.84 (0.2845)	25.87 (0.6110)	25.57 (0.5765)	23.24 (0.4305)	26.08 (0.6566)
Liver	14.48 (0.1653)	23.53 (0.3833)	25.89 (0.5994)	25.52 (0.6048)	23.07 (0.4805)	26.01 (0.6750)
Lung	14.48 (0.1918)	22.68 (0.3503)	24.71 (0.5775)	24.41 (0.5586)	22.17 (0.4880)	24.91 (0.6177)
Spine	14.48 (0.1355)	23.51 (0.4632)	25.59 (0.6367)	25.38 (0.6149)	23.50 (0.4872)	25.79 (0.6943)
Pelvis	14.48 (0.1541)	24.84 (0.3948)	24.86 (0.5841)	24.65 (0.5670)	22.98 (0.5118)	25.04 (0.6046)
PSNR (SSIM) for σ=60						
Abdomen	12.54 (0.1905)	20.79 (0.3476)	22.91 (0.5397)	22.72 (0.5160)	20.92 (0.4567)	23.18 (0.5626)
Brain	12.54 (0.1215)	20.76 (0.2175)	24.44 (0.5165)	24.28 (0.4843)	22.17 (0.3723)	24.85 (0.5693)
Liver	12.54 (0.1270)	21.33 (0.2740)	24.76 (0.5614)	24.28 (0.5320)	22.00 (0.4239)	24.85 (0.6168)
Lung	12.54 (0.1526)	20.48 (0.2655)	23.39 (0.5129)	23.10 (0.4830)	21.08 (0.4369)	23.56 (0.5471)
Spine	12.54 (0.1005)	21.52 (0.3120)	24.56 (0.6086)	24.27 (0.5387)	22.45 (0.4224)	24.77 (0.6367)
Pelvis	12.54 (0.1100)	22.44 (0.2800)	24.90 (0.5305)	23.51 (0.5031)	21.85 (0.4462)	23.95 (0.5493)

SDs – Standard deviations; PSNR – Peak signal to noise ratio; SSIM – Structural similarity; LPG-PCA – Local pixels grouping-principal component analysis; PGPCA – Patch based global PCA; K-LLD – Locally learned dictionaries

REFERENCES

1. Pogossian T. The Physical Aspects of Diagnostic Radiology. New York: Harper & Row, Publishers; 1967.
2. Newton TH, Potts DG. Radiology of the Skull and Brain. Technical Aspects of Computed Tomography. Vol. 5. New York: Academic Press; 1981. p. 3942-54.
3. Kak AC, Slane M. Principles of Computerized Tomographic Imaging, Society of Industrial and Applied Mathematics. USA: IEEE Press; 1988.
4. Donoho DL, Johnstone IM. Adapting to unknown smoothness via wavelet shrinkage. J Am Stat Assoc 1995;90:1200-24.
5. Chang SG, Yu B, Vetterli M. Adaptive wavelet thresholding for image denoising and compression. IEEE Trans Image Process 2000;9:1532-46.
6. Antoniadis A, Bigot J. Wavelet estimators in nonparametric regression: A comparative simulation study. J Stat Softw 2001;6:1-83.
7. Muresan DD, Parks TW. Adaptive Principal Components and Image Denoising. In International Conference on Image Processing; 2003. p. 101-4.
8. Foi A, Katkovnik V, Egiazarian K. Pointwise shape-adaptive DCT for high-quality denoising and deblocking of grayscale and color images. IEEE Trans Image Process 2007;16:1395-411.
9. Zhang L, Dong W, Zhang D, Shi G. Two-stage image denoising by principal component analysis with local pixel grouping. Pattern Recognit 2010;43:1531-49.
10. Muresan DD, Parks TW. Adaptive Principal Components and Image Denoising. In Proceedings of the 2003 International Conference on Image Processing; Vol. 1. 2003. p. I101-4.
11. MacQueen JB. Some Methods for Classification and Analysis of Multivariate Observations. In Proceedings of Berkeley Symposium on Mathematical Statistics and Probability. Berkeley; 1967. p. 281-97.
12. Höppner F, Klawonn F, Kruse R, Runkler T. Fuzzy Cluster Analysis. Chichester: Wiley; 1999.
13. Gersho A. On the structure of vector quantizers. IEEE Trans Inf Theory 1982;28:157-66.
14. Thu H, Ghanbari M. Scope of validity of PSNR in image/video quality assessment. Electron Lett 2008;44:800-1.

15. Wang Z, Bovik AC, Sheikh HR, Simoncelli EP. Image quality assessment: From error visibility to structural similarity. IEEE Trans Image Process 2004;13:600-12.
16. Loza A, Mihyalova L, Canagarajah N, Bull D. Structural Similarity-Based Object Tracking in Video Sequences. Proceedings of the 9th International Conference on Information Fusion; 2006.
17. Chatterjee P, Milanfar P. Clustering-based denoising with locally learned dictionaries. IEEE Trans Image Process 2009;18:1438-51.
18. Charles D, Salmon J, Dalalyam A. Image Denoising with Patch Based PCA: Local Versus Global. 22nd British Machine Vision Conference; 2011.
19. Dabov K, Foi A, Katkovnik V, Egiazarian K. Image denoising by sparse 3-D transform-domain collaborative filtering. IEEE Trans Image Process 2007;16:2080-95.
20. Khanian M, Feizi A, Davari A. An optimal partial differential equations-based stopping criterion for medical image denoising. J Med Signals Sens 2014;4:72-83.
21. Saberkari H, Bahrami S, Shamsi M, Amoshahy MJ, Ghavifekr HB, Sedaaghi MH. Fully automated complementary DNA microarray segmentation using a novel fuzzy-based algorithm. J Med Signals Sens 2015;5:182-91.

BIOGRAPHIES

Mojtaba Fadaee received the B.Sc. degree in Electrical Engineering from Guilan University, Rasht, IRAN, in 2011. In 2014, he received his M.Sc. degree in Communication Engineering from Sahand University of Technology, Tabriz, IRAN. His research interests include De-noising Algorithms, Optimization, and Biomedical Image Processing.

E-mail: m_fadaee@sut.ac.ir.

Mousa Shamsi received his B.Sc. degree in Electrical Engineering (major: Electronics) from Tabriz University, Tabriz, IRAN, in 1995. In 1996, he joined the University of Tehran, Tehran, IRAN. He received his M.Sc. degree in Electrical Engineering (major: Biomedical Engineering) from this university in 1999. From 1999 to 2002, he taught as a lecturer at Sahand University of Technology, Tabriz, Iran. From 2002 to 2008, he was a PhD student at the University of Tehran in Bioelectrical Engineering. In 2006, he was granted with the Iranian government scholarship as a visiting researcher at the Ryukyus University, Okinawa, Japan. From December 2006 to May 2008, he was a visiting researcher at this University. He received his PhD degree in Electrical Engineering (major: Biomedical Engineering) from University of Tehran in December 2008. From December 2008 to April 2013, he was an assistant professor at Faculty of Electrical Engineering, Sahand University of Technology, Tabriz, Iran. From April 2013, he is an associate professor at Faculty of Electrical Engineering, Sahand University of Technology, Tabriz, Iran. His research interests include medical image and signal processing, genomic signal processing, pattern recognition, adaptive networks, and facial surgical planning.

E-mail: shamsi@sut.ac.ir

Hamidreza Saberkari was born in Rasht, Iran. He received the B.Sc. degree in Electrical Engineering from the University of Guilan, Rasht, IRAN, in 2011. In 2013, he received his M.Sc. degree in Communication Engineering from Sahand University of Technology, Tabriz, IRAN. Now, he is a PhD student in Electrical Engineering at Sahand University of Technology, Tabriz, IRAN. He has published more than 20 journal papers and also more than 10 papers in refereed conferences. He is the reviewer of Plos One, IEEE Transactions of Nanobioscience and Applied Medical Informatics journals. From 2014, he is with the Department of Electrical Engineering, Rasht branch, Islamic Azad University, Rasht, Iran and also Department of Electrical Engineering, University of Guilan, Rasht, Iran, as a lecturer. His research interests include optimization algorithms, genomic signal processing, bioinformatics, pattern recognition, Biological Sensors and Bio-MEMS.

E-mail: saberkari@iaurasht.ac.ir

Mohammad Hossein Sedaaghi was born in Tehran, Iran. He received the B.Sc. and M.Sc. degrees from the Sharif University of Technology, Tehran, IRAN, in 1986 and 1987, respectively. In 1998, he received the Ph.D. degree from Liverpool University. He is now a professor at Sahand University of Technology, Tabriz. His research interests include signal/image processing, pattern recognition, machine learning and biometrics.

E-mail: sedaaghi@sut.ac.ir.